

A Method to Minimize Resonant Frequency Drift of CMUTs Due to Fluid Loading

Thasnim Mohammed, Sazzadur Chowdhury
 Department of Electrical and Computer Engineering
 University of Windsor
 Windsor, Ontario, Canada
 e-mail: sazzadur@uwindsor.ca

Abstract— This paper presents a method to minimize the resonant frequency drift of Capacitive Micromachined Ultrasonic Transducers (CMUTs) due to fluid loading. A unified mathematical model for the resonant frequency of a CMUT that includes the electrostatic spring softening effect and the fluid loading effect due to the coupled fluidic layer has been developed that provides the basis of the proposed approach. The minimization method involves dynamic adjustment of the DC bias voltage to modify the electrostatic spring softening parameter to offset the effects of fluid loading. Analytical and COMSOL based 3D Finite Element Analysis (FEA) results show that the drift in the resonant frequency of a 6 MHz CMUT operated in water can be compensated by adjusting the bias voltage by 2% from its 75% pull-in voltage value to render an improvement of 4% in lateral and axial resolutions in imaging applications. A bias voltage adjustment of 9% of the 75% pull-in voltage value is necessary to achieve an improvement of 20.74% when the CMUT is operated in glycerol.

Keywords- CMUT; electrostatic spring softening; fluid loading effect; resonant frequency drift; 3D FEA.

I. INTRODUCTION

Capacitive micromachined ultrasonic transducers are emerging as a superior alternative to piezoelectric transducers for biomedical imaging, Non-Destructive Evaluation (NDE), and High Intensity Focused Ultrasound (HIFU) applications [1]–[3]. They can be batch fabricated using conventional microfabrication techniques at a lower cost and can be efficiently integrated with CMOS based integrated circuits for control, drive, and signal processing to offer improved Signal-to-Noise Ratio (SNR) with higher fractional bandwidth and thermal stability.

The CMUT is basically a reciprocal electrostatic transducer that relies on capacitance change between a movable and a fixed electrode separated by a small gap to generate or receive ultrasound [4][5]. The space between the electrodes is filled with either vacuum or a thin film of air. The movable electrode is supported at the edges by dielectric support posts.

When a CMUT array operates in a fluidic medium, the coupled fluid layer manifests itself as an inertial mass onto the diaphragm and as a viscous damper depending on the viscosity of the fluidic medium. As these fluid loading effects alter the effective mass of the CMUT diaphragm, a drift of the resonant frequency of the CMUT occurs. As the

elements in a CMUT array are designed and fabricated to have a fixed pitch to satisfy the Nyquist criteria of spatial sampling to minimize grating lobes and maximize the main lobe power in beamforming operations, a change in the CMUT resonant frequency compromises the array operation to lower imaging quality.

Serious research is in progress to minimize the fluid loading effects on CMUTs. The fluid loading effects on a circular CMUT cell were investigated in [6], where frequency dependent equivalent density was used as the effective CMUT diaphragm material density to account for the distributed fluid loading. The authors in [6] also presented a dimensional dependence model based on the equivalent density using a finite element method (FEM) based data fitting technique. In another approach [7], linear and nonlinear equivalent circuit models of a CMUT were developed based on electrical, mechanical, and acoustical parameters assuming the CMUT as a piston radiator. The mass loading and waveguiding effects of the fluids were incorporated in the model using data extracted from FEM simulations. The authors in [8] presented a generalized model for surface acoustic wave devices considering the mass and viscous fluid loading. Numerical modeling of fluid interaction with oscillating surfaces is available in [9]. In [10], the sensitivity of a CMUT diaphragm to the dynamic viscosity of the surrounding fluid medium was investigated to realize CMUT based fluid sensors.

In this perspective, this paper presents a method to minimize the resonant frequency drift of a CMUT due to fluid loading by dynamically adjusting the DC bias voltage. The scientific basis of the proposed method lies in the spring softening effect associated with the DC bias voltage applied to a CMUT. Due to an applied DC bias, necessary for CMUT operation in both transmit and receive modes, the effective stiffness of the diaphragm reduces to lower the resonant frequency. As the amount of spring softening (lowering of the stiffness) depends on the DC bias, the DC bias voltage can be dynamically controlled using a suitable microelectronic circuit to adjust the spring softening amount to offset the effect of fluid loading on the resonant frequency. Excellent agreements between lumped element model analysis and 3D electromechanical finite element analysis conducted by the authors show that the method can effectively offset the resonant frequency drift due to fluid loading to validate the hypothesis.

The rest of the paper has been organized in the following

manner: Section II provides the problem statement and theoretical background of the proposed approach, Section III investigates the effect of fluid loading on CMUT resonant frequency in different fluids, Section IV presents the proposed frequency drift compensation method with simulation results of analytical and FEA analysis using COMSOL and finally, Section V provides the concluding remarks.

II. THEORETICAL BACKGROUND

A CMUT array is comprised of several transmit and receive elements as shown in Figure 1(a). Each element in turn is designed to have several CMUT cells connected in parallel [9][11]-[14]. A conceptual cross-section of a typical CMUT cell is shown in Figure 1(b).

Assuming that the stiffness of the diaphragm is linear, the resonant frequency of a CMUT in air can be calculated following

$$f_{\text{res}} = \frac{1}{2\pi} \sqrt{\frac{k}{m}} \quad (1)$$

where, k and m are the stiffness and mass of the CMUT diaphragm as shown in Figure 1(b), respectively. Typically, the CMUT diaphragms are constructed to have a circular, hexagonal, or square shape geometry to satisfy the design requirements.

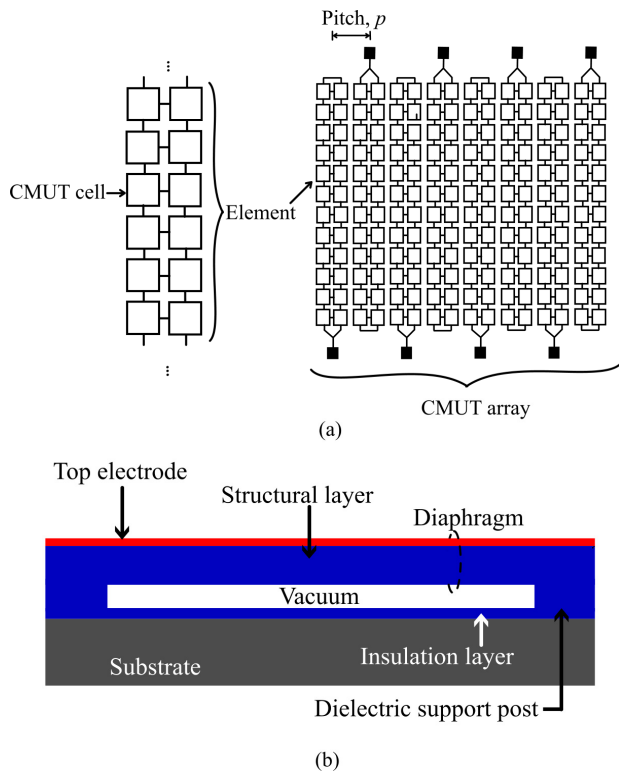


Figure 1. (a) Layout of a CMUT array comprising of array elements. (b) Typical cross-section of a single CMUT cell.

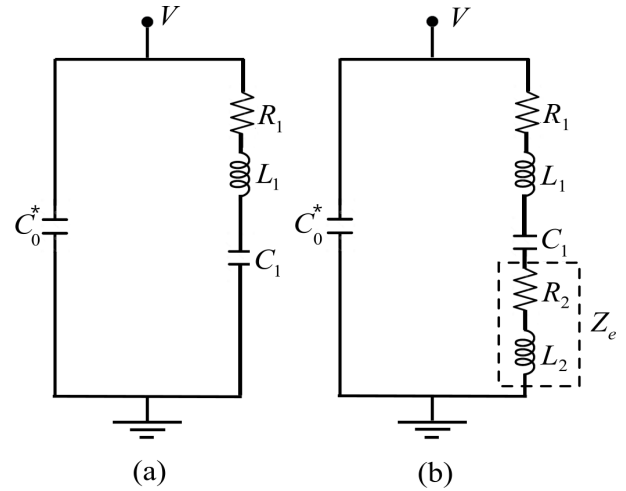


Figure 2. (a) The BVD model of a CMUT without fluid loading. (b) The BVD model of a CMUT with fluid loading. The fluid loading effect is represented by inductance L_2 and resistance R_2 .

The array pitch, defined as the distance between corresponding points in the neighboring elements (Figure 1(a)), is optimized following Nyquist criteria of spatial sampling to minimize grating lobes following

$$p \leq \frac{\lambda}{2} \quad (2)$$

where, λ is the wavelength corresponding to the center frequency of operation.

The frequency response of a CMUT cell with and without the fluid loading effect can be obtained using the Butterworth-Van Dyke (BVD) model as shown in Figure 2(a) [15]. The BVD model depicts an analog electrical equivalent circuit of a CMUT that includes both electrical and equivalent mechanical lumped element circuit parameters.

In the BVD model, the electrical circuit element is represented by a lumped capacitor C_0^* , and the electrical equivalent of mass m , stiffness k , and damping element b is represented by L_1 , C_1 , and R_1 respectively. Assuming that the CMUT diaphragm is square, the stiffness k of the diaphragm can be calculated following

$$k = C_r \frac{t_d \sigma_0}{(L/2)^2} + C_b \frac{12D_{\text{eff}}}{(L/2)^4} \quad (3)$$

where $C_r = 3.45$ and $C_b = 4.06$ [16]. The parameters D_{eff} , L , σ_0 , and t_d are the effective flexural rigidity, sidelength, residual stress, and thickness of the diaphragm, respectively. The mass of the diaphragm can be calculated from the volume and density of the CMUT diaphragm materials. The parameters R_1 , L_1 , and C_1 (zero bias equivalent stiffness) can be calculated from [15] following

$$\left. \begin{aligned} C_1 &= \frac{n^2}{k} \\ L_1 &= \frac{m}{n^2} \\ R_1 &= \frac{b}{n^2} \end{aligned} \right\} \quad (4)$$

where, n is the electromechanical transformation ratio.

The coupling of the CMUT diaphragm with a liquid medium alters the CMUT motional impedance contributed by L_1 , C_1 , and R_1 . The adjacent (coupled) liquid layer contributes an additional equivalent damping R_2 due to the fluid viscosity and an additional equivalent fluid mass L_2 . The inclusion of these additional mass and damping parameters in the BVD model as shown in Figure 2(b) alters the frequency response of the CMUT. The amount of alteration (drift) depends on the density and viscosity of the fluidic medium.

Following [15], the fluid loading quantities L_2 and R_2 can be approximately calculated from

$$L_2 = \frac{\pi}{4k_s^2 \omega_s C_0} \left(\frac{\rho \eta}{2\omega_s \mu_q \rho_q} \right)^{\frac{1}{2}} \quad (5)$$

$$R_2 = \frac{\pi}{4k_s^2 C_0} \left(\frac{\rho \eta}{2\omega_s \mu_q \rho_q} \right)^{\frac{1}{2}} \quad (6)$$

where, ρ , η , μ_q , ρ_q , k_s^2 and ω_s represents the liquid density, shear viscosity of the liquid, diaphragm shear stiffness, mass density of diaphragm, coupling coefficient, and resonant frequency of the circuit in rad/sec, respectively.

The entrained liquid layer of effective height $\delta/2$ is considered for the calculations shown in (5)–(6) where $\delta = \sqrt{2\eta / \omega_s \rho}$ is the depth of penetration of damped shear wave propagating into the liquid by the oscillating surface [15][17]. Thus, the motional impedance Z_m in the BVD model of a CMUT including the fluid loading effect (Figure 2(b)) can be expressed as:

$$Z_m = R_1 + R_2 + j\omega L_1 + j\omega L_2 + \frac{1}{j\omega C_1} \quad (7)$$

On the other hand, assuming the small-signal model of a CMUT where the AC actuation signal is much smaller compared to the DC bias voltage ($V_{DC} \gg V_{AC}$), the spring softening effect due to the applied DC bias voltage reduces the zero bias CMUT diaphragm stiffness k by a factor k_{soft} as given by (8).

$$k_{\text{soft}} = \frac{\epsilon A V_{DC}^2}{d_{\text{eff}}^3} \quad (8)$$

where, ϵ , A , V_{DC} , and d_{eff} denote the permittivity, coupling area of the electrodes, DC bias voltage applied to the CMUT, and the effective electrode gap, respectively. Consequently, the spring softening effect causes a downshift of the resonant frequency of the CMUT diaphragm following

$$f_{\text{res-ss}} = \frac{1}{2\pi} \sqrt{\frac{k - k_{\text{soft}}}{m}} \quad (9)$$

During an immersion operation, the resonant frequency $f_{\text{res-ss}}$ as expressed in (9) is further affected by the inertial mass m_f contributed by the coupled fluid layer adjacent to the CMUT diaphragm.

Thus, including both the spring softening effect and the fluid loading effect, the resonant frequency $f_{\text{res-ss-fl}}$ of the diaphragm can be expressed as

$$f_{\text{res-ss-fl}} = \frac{1}{2\pi} \sqrt{\frac{k - k_{\text{soft}}}{m + m_f}} \quad (10)$$

A careful examination of (8) and (10) reveals that the drift in the resonant frequency due to the fluid loading effect m_f alone can be minimized by adjusting the spring softening factor k_{soft} which is a function of the bias voltage V_{DC} in small-signal approximation.

A suitable microelectronic circuit can be used to sense the resonant frequency offset and adjust the bias voltage dynamically to control k_{soft} to bring the resonant frequency back to its design value while generating the desired acoustic pressure.

III. INVESTIGATION OF FLUID LOADING EFFECTS

A. Analytical CMUT Resonant Frequency Calculation with Fluid Loading Effects

To investigate the proposed approach, a linear CMUT array with a center frequency of 6 MHz has been considered. This center frequency is suitable for cardiac diagnostic imaging as reported in [18]. Individual CMUT cells in the array have been designed to have the same resonant frequency as the array [19]. The element pitch p has been selected following (2) to satisfy the Nyquist criteria of spatial sampling to obtain better directivity with minimum side lobes. The lateral and axial resolution of the CMUT array is given by [1] as:

$$\Delta y = \left(\frac{1.22\lambda}{A_a} \right) S \quad (11)$$

$$\Delta x = \frac{n\lambda}{2} \tag{12}$$

respectively, where, A_a , S and n are the array aperture, the distance between the focus and the array surface at the center of the array, and the number of scanning pulses, respectively. Following (11) and (12), it is necessary for the CMUT and the array physical dimensions to correspond to the same wavelength or center frequency to achieve setpoint axial and lateral resolutions and avoid any deviation from Nyquist criteria of spatial sampling [20][21].

To investigate the effects of viscosity and density of the fluidic medium on the resonant frequency of the CMUT diaphragms, a square shaped CMUT diaphragm with the same 6 MHz center frequency in air as for the array has been investigated.

Typical CMUT diaphragms are fabricated as a multilayer laminate where a thin insulating material is used as the structural layer to provide the necessary mechanical strength and a thin conducting layer is used on the top of the structural layer to enable electrical functionality.

Following [20], bisbenzocyclobutene (BCB) has been used as the structural layer for this analysis. The BCB layer is coated with a thin layer of gold to form the top electrode. Low resistivity silicon has been used to constitute the ground electrode. BCB has also been used to fabricate the dielectric support post. The major physical properties of the selected CMUT materials are listed in Table I.

To obtain the 6 MHz resonant frequency in air using the materials listed in Table I, a diaphragm sidelength of 28 μm , BCB layer thickness of 1.5 μm , and gold layer thickness of 0.1 μm has been determined following [22].

The pull-in voltage of the CMUT has been determined from 3D electromechanical FEA using COMSOL as 395 volts. The frequency responses of the CMUT biased at 295 volts (74.68% of the pull-in voltage) in air, water, engine oil, and glycerol are shown in Figure 3. The physical properties of the fluids are listed in Table II.

The frequency response in air without any DC bias voltage has also been shown in Figure 3. As it can be seen, there is a significant drift in the resonant frequency due to the spring softening effect caused by the bias voltage which

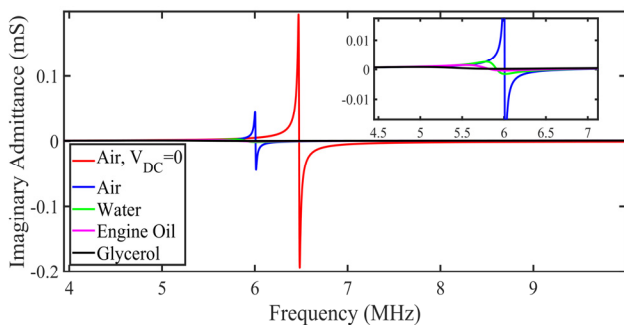


Figure 3. Frequency response of the CMUT cell with bias voltage $V_{DC} = 0.75V_{PI}$ for unloaded (air) and loaded (water, engine oil, glycerol) conditions. (Inset y-axis unit is in μS .)

TABLE I. CMUT MATERIAL PROPERTIES

Material	Young's modulus (GPa)	Poisson's ratio	Density (kg.m^{-3})	Residual stress (MPa)
BCB	2.9	0.34	1050	28
Gold	70	0.44	19300	106
Silicon	165.9	0.26	2329	55

TABLE II. CMUT RESONANT FREQUENCIES IN INVESTIGATED FLUIDS

Fluid type	Fluid Physical Properties		Resonant frequency (MHz)
	Viscosity (mPa/s)	Density (g/cm^3)	
Air	0.01825	0.001204	6.002
Water	1.0016	0.998	5.783
Engine oil	287.23	0.8787	5.422
Glycerol	1412.8	1.2608	4.975

is further deteriorated by the fluid loading effects contributed by the fluid mass and viscosity as shown in the zoomed-up inset.

B. 3D FEA Based CMUT Resonant Frequency Simulation with Fluid Loading Effects

A 3D FEA of a single CMUT cell was conducted in COMSOL Multiphysics environment to investigate the fluid loading effects on the frequency response of the CMUT cell. The cell was modeled using the electro-mechanical module as shown in Figure 4. The air/fluid column was designed using the pressure acoustics frequency domain physics module.

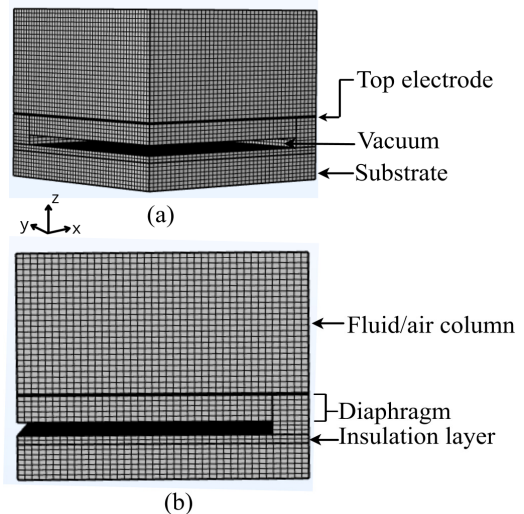


Figure 4. The CMUT model in COMSOL (As the structure is symmetric, only a quarter model of the CMUT was simulated).

The CMUT diaphragm was set as a linear elastic material and necessary boundary conditions were applied. The boundary between the electro-mechanics and pressure acoustics domain was defined as a fluid-solid coupled boundary that acts as a pressure load on the electro-mechanics domain. The maximum element size was set to one-sixth of the smallest wavelength in a frequency sweep while meshing. An AC perturbation signal superimposed with DC bias voltage was applied to the CMUT cell using the default frequency domain modal analysis method in COMSOL.

The COMSOL based 3D FEA generated modal frequency responses of the CMUT model for the fluids listed in Table II are shown in Figure 5.

Table III compares the analytical and 3D FEA results for the resonant frequencies of the CMUT in the investigated fluids. As it can be seen from Table III, the analytical and 3D FEA results are in excellent agreement with a maximum deviation of 2.8% for the liquids that validate the efficacy of the analytical and simulation methods.

IV. MINIMIZING THE FLUID LOADING EFFECTS

The resonant frequency drift due to the fluid loading effect as confirmed by the analytical and 3D FEA based analysis can be minimized by adjusting the DC bias voltage following (8) and (10). The spring softening parameter k_{soft} as expressed in (8) needs to be dynamically adjusted by controlling the bias voltage V_{DC} , to offset the fluid loading effect induced resonant frequency drift Δf expressed in (13).

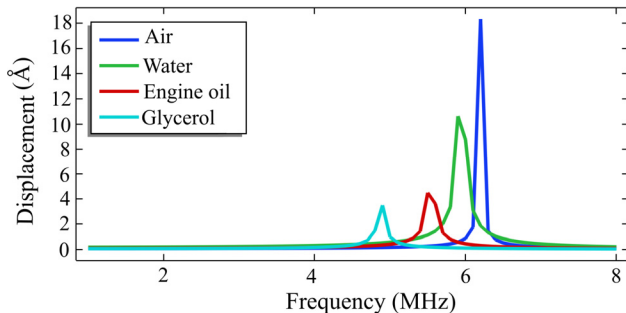


Figure 5. FEA simulation based frequency response of the CMUT cell in different fluids.

TABLE III. RESONANT FREQUENCY OF THE SIMULATED CMUT IN DIFFERENT FLUIDS

Medium	Resonant frequency (Analytical) (MHz)	Resonant frequency (FEA) (MHz)	Percentage deviation between analytical and FEA (%)	Drift from the resonant frequency in air (FEA)(%)
Air	6.002	6.19	3.1	-
Water	5.783	5.945	2.8	3.9
Engine oil	5.422	5.545	2.3	10.42
Glycerol	4.975	4.8788	1.9	21.18

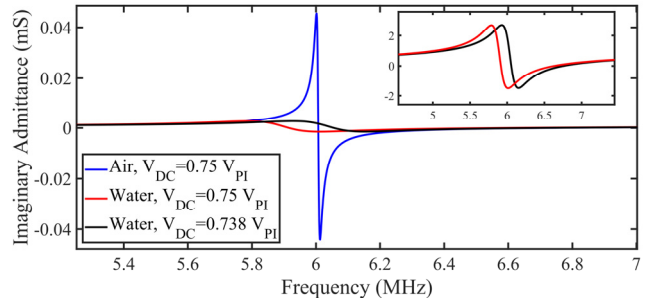


Figure 6. Simulation result of CMUT small-signal analysis for frequency compensation in water. (Inset y-axis unit is in μS .)

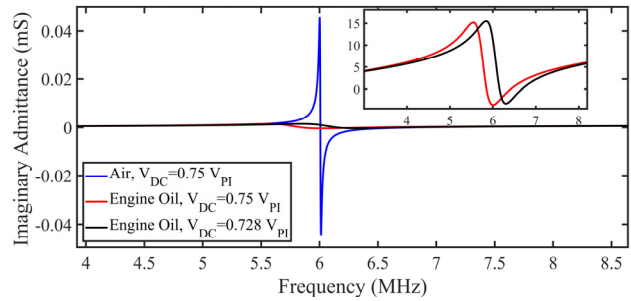


Figure 7. Simulation result of CMUT small-signal analysis for frequency compensation in engine oil. (Inset y-axis unit is in μS .)

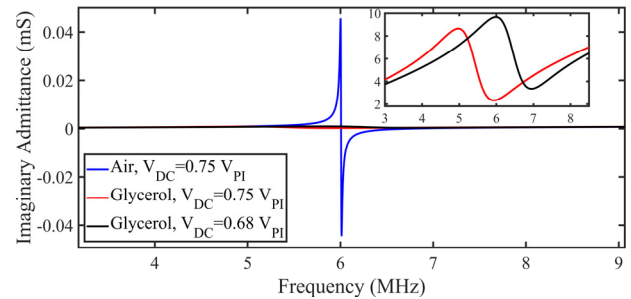


Figure 8. Simulation result of CMUT small-signal analysis for frequency compensation in glycerol. (Inset y-axis unit is in μS .)

$$\Delta f = f_{res} - f_{res-ss-fl} \tag{13}$$

COMSOL based 3D FEA simulation results after adjusting the bias voltage to offset the resonant frequency drift Δf for water, engine oil, and glycerol are shown in Figures 6–8. The reference bias voltage was kept at 75% of the pull-in voltage V_{PI} of the CMUT structure as in the previous section. When the CMUT was operated in water, engine oil, and glycerol, the change in bias voltage applied was 2%, 4.2%, and 9% respectively (Figures 6–8). The simulation results confirm that the drift Δf in the resonant frequency can effectively be compensated by a small change in the DC bias V_{DC} to validate the hypothesis.

The improvement in the lateral and axial resolution that could be achieved with the proposed method is 4%, 10.78%, 20.74% when operated in water, engine oil, or glycerol,

respectively. Thus, the proposed method will help to achieve the expected resolution even when the array is operated in different fluidic mediums, thereby improving the imaging accuracy of a CMUT array.

V. CONCLUSION AND FUTURE WORK

This paper presented a method to minimize the fluid loading induced resonant frequency drift of a CMUT by dynamically adjusting the bias voltage. Analytical and 3D FEA based simulation studies revealed that the amount of change in DC bias voltage necessary to offset the resonant frequency drift is small and is not expected to affect the acoustic power/pressure output of a CMUT array. The investigation shows that the method can improve the lateral and axial resolutions in water by approximately 4% to improve the accuracy of CMUT based biomedical diagnostic imaging. For NDE applications, the axial and lateral resolution improvements can be as high as 20.74% when glycerol is used as the coupling agent.

The design of a high-speed microelectronic control circuit necessary to implement the proposed scheme is in progress. In the currently investigated scheme, the received signal is signal-conditioned first to remove noise and other high frequency components. A high-speed data converter with a desired sampling rate is used to digitize the actuating AC signal and the received signal. Fast Fourier Transform (FFT) of the transmit and the processed received signal provides the frequency components necessary to calculate Δf . Thus, the frequency drift Δf is measured in real time to determine the DC bias voltage necessary to be adjusted to offset the resonant frequency drift.

ACKNOWLEDGMENT

This research work was supported by the Natural Science and Engineering Research Council of Canada (NSERC)'s discovery grant number RGPIN 293218. The authors also acknowledge the collaborative research support provided by the IntelliSense Corporation, Lynnfield, MA, Angstrom Engineering, ON, and the CMC Microsystems, Canada.

REFERENCES

[1] J. Song et al. "Capacitive Micromachined Ultrasonic Transducers (CMUTs) for Underwater Imaging Applications," *Sensors*, vol. 15, no. 9, pp. 23205–23217, Sep. 2015.

[2] D. Zhao, S. Zhuang, and R. Daigle, "A Commercialized High Frequency CMUT Probe for Medical Ultrasound Imaging," in *Proc. of 2015 IEEE International Ultrasonics Symposium (IUS)*, Oct. 21-24, Taipei, Taiwan, 2015, pp. 1-4.

[3] A. S. Ergun, G. G. Yaralioglu, O. Oralkan, and B. T. Khuri-Yakub, "Chapter 7: Techniques & Applications of Capacitive Micromachined Ultrasonic Transducer," in *MEMS/ NEMS Handbook [Techniques and Applications]*; Leondes, C.T., Ed.; Springer Science + Business Media Inc.: Los Angeles, CA, USA, 2006; Volume 2, pp. 222–332.

[4] A. S. Ergun, G. G. Yaralioglu, and B. T. Khuri-Yakub, "Capacitive Micromachined Ultrasonic Transducers: Theory and Technology." *Journal of Aerospace Engineering*, vol 16, no. 2, pp. 76-84, 2003.

[5] Y. Huang, A. S. Ergun, E. Haeggstrom, M. H. Badi, and B. T. Khuri-Yakub, "Fabricating Capacitive Micromachined Ultrasonic

Transducers with Wafer-bonding Technology," *Journal of Microelectromechanical Systems*, vol. 12, no. 2, pp. 128-137, April 2003.

[6] B. Azmy, M. El-Gamal, A. El-Henawy, and H. Ragai, "An Accurate Model for Fluid Loading on Circular CMUTs," in *Proc. of 2011 IEEE International Ultrasonics Symposium*, Orlando, Florida, Oct. 18-24, 2011, pp. 584-587.

[7] A. Lohfink, P. -. Eccardt, W. Benecke, and H. Meixner, "Derivation of a 1D CMUT Model from FEM Results for Linear and Nonlinear Equivalent Circuit Simulation," in *Proc. of 2003 IEEE Ultrasonics Symposium*, Honolulu, Hawaii, Oct. 5-8, 2003 pp. 465-468.

[8] M. Tsai and J. Jeng, "Development of a Generalized Model for Analyzing Phase Characteristics of SAW Devices Under Mass and Fluid Loading," in *IEEE Trans. on Ultrasonics, Ferroelectrics, and Frequency Control*, vol. 57, no. 11, pp. 2550-2563, November 2010.

[9] E. K. Reichel, M. Heinisch, B. Jakoby, and T. Voglhuber-Brunnmaier, "Efficient Numerical Modeling of Oscillatory Fluid-Structure Interaction," in *Proc. of IEEE SENSORS 2014*, Valencia, Spain, Nov. 2-5, 2014, pp. 958-961,

[10] M. Thränhardt, P. Eccardt, H. Mooshofer, P. Hauptmann, and L. Degertekin, "A Resonant CMUT Sensor for Fluid Applications," in *Proc. of IEEE SENSORS 2009*, Christchurch, New Zealand, 25-28 October, 2009, pp. 878-883.

[11] H. Wang, X. Wang, C. He, and C. Xue, Design and Performance Analysis of Capacitive Micromachined Ultrasonic Transducer Linear Array. *Micromachines*, vol. 5, no. 3, pp.420-431, 2014.

[12] T. Zure, "Characterization of a CMUT Array," Master's Thesis, Dept. of Electrical and Computer Engineering, Univ. of Windsor, Windsor, ON, Canada, 2012.

[13] V. Yashvanth, "CMUT Crosstalk Reduction Using Crosslinked Silica Aerogel," Master's Thesis, Dept. of Electrical and Computer Engineering, Univ. of Windsor, Windsor, ON Canada, 2018.

[14] R. Zhang et al. "Design and Performance Analysis of Capacitive Micromachined Ultrasonic Transducer (CMUT) Array for Underwater Imaging." *Microsystem Technologies*, vol. 22, no. 12, pp. 2939-2947, 2016.

[15] D. S. Ballantine Jr et al. *Acoustic wave sensors: theory, design and physico-chemical applications*. San Diego, CA, USA: Elsevier; 1996.

[16] M. Rahman and S. Chowdhury, "A New Deflection Shape Function for Square Membrane CMUT Design," in *Proc. of 2010 IEEE International Symposium on Circuits and Systems (ISCAS2010)*, Paris, France, 2010, pp. 2019-2022.

[17] S. J. Martin, Gregory C. Frye, Antonio J. Ricco, and Stephen D. Senturia, "Effect of Surface Roughness on the Response of Thickness-shear Mode Resonators in liquids," *Analytical Chemistry*, vol. 65, pp. 2910-2922, 1993.

[18] E. Ashley, J. Niebauer, *Cardiology Explained*. London: Remedica; 2004. Chapter 4, Understanding the Echocardiogram. [Online]. Available: <https://www.ncbi.nlm.nih.gov/books/NBK2215/> [retrieved: August, 2021].

[19] M. Rahman, J. Hernandez, and S. Chowdhury, "An Improved Analytical Method to Design CMUTs with Square Diaphragms," in *IEEE Transactions on Ultrasonics, Ferroelectrics, and Frequency Control*, vol. 60, no. 4, pp. 834-845, April 2013.

[20] R. Manwar, "A BCB Diaphragm Based Adhesive Wafer Bonded CMUT Probe for Biomedical Application," Ph.D. dissertation, Dept. of Electrical and Computer Engineering, Univ. of Windsor, Windsor, ON, Canada, 2017.

[21] F. Pavlo, "Capacitive Micromachined Ultrasonic Transducer (cMUT) for Biometric Applications," Master's Thesis, Dept. of Nanoscience and Technology, Chalmers University of Technology, Göteborg, Sweden, 2012.

[22] R. Manwar, L. Arjunan, M. Ahmadi, and S. Chowdhury, "Resonant Frequency Calculation of Square Diaphragms: A Comparison," in *Proc of IEEE 6th Latin American Symposium on Circuits & Systems (LASCAS)*, Montevideo, Uruguay, Feb. 24-27, 2015, pp. 1-4.